

# A Fill Factor Loss Analysis Method for Silicon Wafer Solar Cells

Ankit Khanna, Thomas Mueller, Rolf A. Stangl, Bram Hoex, Prabir K. Basu, and Armin G. Aberle

**Abstract**—The fill factor of silicon wafer solar cells is strongly influenced by recombination currents and ohmic resistances. A practical upper limit for the fill factor of crystalline silicon solar cells operating under low-level injection is set by recombination in the quasi-neutral bulk and at the two cell surfaces. Series resistance, shunt resistance, and additional recombination currents further lower the fill factor. For process optimization or loss analysis of solar cells, it is important to determine the influence of both ohmic and recombination loss mechanisms on the fill factor. In this paper, a method is described to quantify the loss in fill factor due to series resistance, shunt resistance, and additional recombination currents. Only the 1-Sun  $J$ - $V$  curve, series resistance at the maximum power point, and shunt resistance need to be determined to apply the method. Application of the method is demonstrated on an 18.4% efficient inline-diffused p-type silicon wafer solar cell and a 21.1% efficient heterojunction n-type silicon wafer solar cell. Our analysis does not require  $J$ - $V$  curve fitting to extract diode saturation current densities or ideality factor; however, the results are shown to be consistent with curve fitting results if the cell's two-diode model parameters can be unambiguously determined by curve fitting.

**Index Terms**—Crystalline silicon solar cells, fill factor, ohmic losses, recombination losses.

## I. INTRODUCTION

FOR silicon wafer solar cells, it is extremely important to achieve high fill factors to maximize the power generation capabilities of the cell. The fill factor of silicon wafer solar cells is strongly influenced by recombination currents and ohmic resistances. To account for these effects, the two-diode model of solar cells [1] is commonly used, which includes two diodes with saturation current densities  $J_{01}$ ,  $J_{02}$ , and ohmic resistors  $R_s$ ,  $R_{sh}$  in series and parallel to the diodes, respectively (see Fig. 1). The  $J_{01}$  diode describes recombination currents in the quasi-neutral bulk and the two cell surfaces.  $J_{02}$  recombination is most commonly attributed to SRH recombination [2], [3] in the space charge regions of the cell and an ideality factor  $n_2 = 2$  is sometimes assigned to the  $J_{02}$  diode from SRH statistics [4],

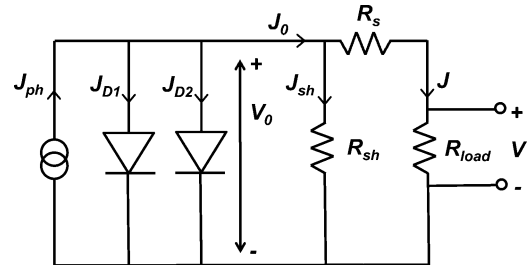


Fig. 1. Schematic of the two-diode model of a solar cell.

although deviations from this theoretical expectation have also been reported. Other proposed sources of  $J_{02}$  recombination are edge recombination [5] and recombination at localized regions with a high defect density [6], [7] which may lead to  $n_2 > 2$ . In this paper, we will refer to all recombination currents which do not follow the ideal-diode behavior as  $J_{02}$  recombination and treat  $n_2$  as a variable cell parameter. Equation (1), shown below, represents the  $J$  ( $V$ ) equation for the two-diode model of solar cells

$$J = J_{ph} - J_{01}[\exp\{q(V + JR_s)/kT\} - 1] - J_{02}[\exp\{q(V + JR_s)/n_2kT\} - 1] - (V + JR_s)/R_{sh}. \quad (1)$$

We present a method to quantify the loss in fill factor for silicon wafer solar cells operating under low-level injection (LLI) due to series resistance, shunt resistance, and  $J_{02}$  recombination, based on the two-diode model. As a first step, a practical upper limit of fill factor is determined by assuming the absence of  $R_s$ ,  $R_{sh}$ , and  $J_{02}$ . Since the fill factor in this case depends on  $J_{01}$  recombination, we call it the “ $J_{01}$  limit” of fill factor. In subsequent steps, we quantify the losses in fill factor due to  $R_s$ ,  $R_{sh}$ , and  $J_{02}$ . Greulich *et al.* [8] and Hoenig *et al.* [9] have previously proposed using the difference between the  $J_{01}$  limit of fill factor and the pseudo fill factor, measured by the Suns- $V_{oc}$  method [10], to quantify fill factor loss due to space charge region recombination. However, this approach is valid only if the effect of shunt resistance is negligible. In general, it is useful to consider the effects of a finite shunt resistance for an accurate loss analysis, especially for cells with high  $V_{oc}$ . Our fill factor loss analysis does not involve fitting procedures to extract  $J_{01}$ ,  $J_{02}$ , and  $n_2$ . The motivation for avoiding fitting procedures is to avoid assumptions about  $n_2$ . As mentioned earlier, the sources of  $J_{02}$  need not strictly follow an ideality factor of 2. In addition, the  $J_{02}$  recombination of a solar cell can arise from more than one source, and each  $J_{02}$  contributor may have a different ideality factor, which would again complicate fitting

Manuscript received January 21, 2013; revised April 30, 2013; accepted May 27, 2013. Date of publication July 9, 2013; date of current version September 18, 2013. The Solar Energy Research Institute of Singapore is sponsored by the National University of Singapore and Singapore's National Research Foundation (NRF) through the Singapore Economic Development Board. This work was supported by the NRF under Grant NRF2010EWT-CERP001-022.

The authors are with the Solar Energy Research Institute of Singapore, Singapore 117574 (e-mail: ankit.khanna@nus.edu.sg; thomas.mueller@nus.edu.sg; rolf.stangl@nus.edu.sg; bram.hoex@nus.edu.sg; prabir.basu@nus.edu.sg; armin.aberle@nus.edu.sg).

Color versions of one or more of the figures in this paper are available online at <http://ieeexplore.ieee.org>.

Digital Object Identifier 10.1109/JPHOTOV.2013.2270348

procedures. Hence, the method proposed here is independent of the ideality factor of the  $J_{02}$  current and directly quantifies the lumped effect of all  $J_{02}$  sources on fill factor. Only the 1-Sun  $J$ - $V$  curve, series resistance at MPP, and shunt resistance need to be determined to apply the method. The method is discussed in the next section, followed by a rigorous analysis of the method's approximations. The method is demonstrated on an 18.4% efficient inline diffused p-type silicon wafer solar cell and a 21.1% efficient heterojunction n-type silicon wafer solar cell.

## II. FILL FACTOR LOSS ANALYSIS METHOD

### A. $J_{01}$ Limit of Fill Factor

The  $J_{01}$  limit of fill factor ( $FF_{J01}$ ) is determined by assuming the absence of  $R_s$ ,  $R_{sh}$ , and  $J_{02}$ . In this case, (1) reduces to

$$J = J_{ph} - J_{01} [\exp(qV/kT) - 1]. \quad (2)$$

Imposing the conditions  $J = 0$  at  $V = V_{oc}$  and  $J = J_{sc}$  at  $V = 0$ , (2) takes the form:

$$J = J_{sc} - \frac{J_{sc}}{\exp(qV_{oc}/kT) - 1} [\exp(qV/kT) - 1]. \quad (3)$$

The fill factor of the  $J$ - $V$  curve given by (3) is  $FF_{J01}$ . This procedure is used in this paper to determine  $FF_{J01}$ , but it is useful to also discuss analytical methods to determine  $FF_{J01}$ .  $FF_{J01}$  can be approximated analytically using the empirical formula proposed by Green [11]. Another method to obtain  $FF_{J01}$  is to use the Lambert W-Function [12]  $W$ , which provides an exact solution (derivation in the appendix) as stated in (4), although mathematical software is needed to evaluate the Lambert W-Function. For the cells analyzed in this paper,  $FF_{J01}$  determined by all three approaches discussed here matched within 0.01% absolute (for  $FF_{J01}$  in %)

$$FF_{J01} = \frac{kT}{qV_{oc}} \cdot \frac{(W[z] - 1)^2 \exp(W[z] - 1)}{\exp(qV_{oc}/kT) - 1} \quad (4)$$

$$z = \exp[1 + qV_{oc}/kT].$$

To apply the next steps of the fill factor loss analysis, we make an approximation that  $R_s$ ,  $R_{sh}$ , and  $J_{02}$  do not influence  $J_{sc}$  or  $V_{oc}$ . For  $R_s$  and  $R_{sh}$ , this approximation is valid within the range of these resistances determined in Section III-B (for the validity of a separate approximation introduced in the next step); therefore, the influence of  $R_s$  and  $R_{sh}$  on  $J_{sc}$  and  $V_{oc}$  is not separately discussed. While  $J_{02}$  affects both  $V_{oc}$  and  $FF$ , at high voltages the  $J_{01}$  current dominates the cell's electrical characteristics and the effect of  $J_{02}$  on  $V_{oc}$  is small. We will revisit this approximation in Section III-A.

### B. Fill Factor Loss due to $R_s$ and $R_{sh}$

Considering the two-diode model at MPP (see Fig. 1), the terminal voltage and current density (subscript mpp added to  $V$  and  $J$ ) will be related to  $R_s$  and  $R_{sh}$  by

$$V_{mpp} = V_0 - J_{mpp} R_s \quad (5)$$

$$J_{mpp} = J_0 - (V_{mpp} + J_{mpp} R_s)/R_{sh}. \quad (6)$$

From (5) and (6), the product  $V_0 J_0$  can be determined and normalized with  $V_{oc} J_{sc}$  to obtain

$$\frac{V_0 J_0}{V_{oc} J_{sc}} = \frac{V_{mpp} J_{mpp}}{V_{oc} J_{sc}} + \frac{J_{mpp}^2 R_s}{V_{oc} J_{sc}} + \frac{(V_{mpp} + J_{mpp} R_s)^2}{R_{sh} V_{oc} J_{sc}}. \quad (7)$$

We make an approximation here that  $V_0$ ,  $J_0$  is the MPP of the resistance-free cell. This is equivalent to the approximation that  $R_s$  only shifts  $V_{mpp}$  and  $R_{sh}$  only shifts  $J_{mpp}$ . In general,  $V_0$ ,  $J_0$  will not be the MPP of the resistance-free solar cell; however, it will be sufficiently close to the MPP for a range of  $R_s$  and  $R_{sh}$ . The error due to this approximation is discussed in Section III-B. Under this approximation, the fill factor of the resistance-free cell  $FF_0$  will be related to the fill factor of the real cell  $FF$  by

$$FF_0 = FF + \frac{J_{mpp}^2 R_s}{V_{oc} J_{sc}} + \frac{(V_{mpp} + J_{mpp} R_s)^2}{R_{sh} V_{oc} J_{sc}}. \quad (8)$$

The second and third terms on the right-hand side of (8) are the fill factor losses due to  $R_s$  and  $R_{sh}$ :  $\Delta FF_{Rs}$  and  $\Delta FF_{Rsh}$ . Since we obtain these terms at MPP using measured  $R_s$  at MPP, no error is expected due to distributed resistance effects [13]

$$\Delta FF_{Rs} = J_{mpp}^2 R_s / V_{oc} J_{sc} \quad (9)$$

$$\Delta FF_{Rsh} = (V_{mpp} + J_{mpp} R_s)^2 / R_{sh} V_{oc} J_{sc}. \quad (10)$$

### C. Fill Factor Loss due to $J_{02}$ Recombination

The loss in fill factor due to  $J_{02}$  recombination,  $\Delta FF_{J02}$ , is the difference between the  $J_{01}$  limit of fill factor,  $FF_{J01}$ , and the resistance free fill factor,  $FF_0$ . Thus, (9)–(11) specify the fill factor loss due to  $R_s$ ,  $R_{sh}$ , and  $J_{02}$  recombination

$$\Delta FF_{J02} = FF_{J01} - FF_0. \quad (11)$$

## III. ERROR ANALYSIS

We will now analyze the approximations made in the previous section individually to obtain a range of  $R_s$ ,  $R_{sh}$ , and  $J_{02}$  for which the error is within acceptable limits.

### A. Approximation: $J_{02}$ Recombination Does Not Influence $V_{oc}$

If the effect of  $J_{02}$  on  $V_{oc}$  is neglected, and the measured  $V_{oc}$  (which includes the influence of  $J_{02}$ ) is used to determine  $FF_{J01}$ , then  $FF_{J01}$  will be underestimated. Since the resistance corrected fill factor  $FF_0$  includes the effect of  $J_{02}$  recombination, this approximation does not introduce an error in  $FF_0$ . Thus, from (11),  $\Delta FF_{J02}$  will also be underestimated. To analyze this error, we define two sets of baseline (one-diode ideal) simulation parameters summarized in Table I. Baseline 1 represents a typical diffused-emitter p-type silicon wafer solar cell, and Baseline 2 represents a high-efficiency n-type silicon wafer solar cell. For Baseline 2,  $V_{oc}$  and  $J_{sc}$  reported in [14] are used as an approximate reference.

The drop in  $V_{oc}$  when a  $J_{02}$  term (taking  $n_2 = 2$ ) is introduced to the baseline models is shown in Fig. 2 (top). It is clear that cells with higher  $V_{oc}$  will be affected more strongly by the presence of  $J_{02}$  recombination. The relative error in  $\Delta FF_{J02}$

TABLE I  
BASELINE PARAMETERS USED TO DETERMINE THE ERROR IN  $FF_{J01}$

Description	Cell parameter	Baseline 1 (standard cell)	Baseline 2 (high-eff. cell)
Simulation input parameter	$J_{01}$ (A/cm <sup>2</sup> )	$1 \times 10^{-12}$	$2.5 \times 10^{-14}$
	$J_{ph}$ (mA/cm <sup>2</sup> )	37.0	40.5
Resulting cell parameter	$V_{oc}$ (mV) for $J_{02}=0$	625.3	722.4
	$FF_{J01}$ (%)	83.3	85.0

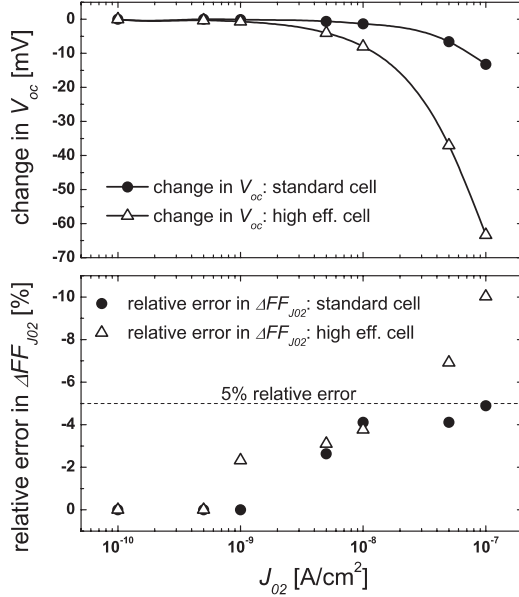


Fig. 2. (Top) Change in  $V_{oc}$  as a function of  $J_{02}$  according to a two-diode simulation for the baseline parameters in Table I. (Bottom) Relative error in  $\Delta FF_{J02}$  as a function of  $J_{02}$ . Top and bottom graphs have the same x-axis.

is shown in Fig. 2 (bottom). The negative sign indicates that  $\Delta FF_{J02}$  is underestimated. It can be seen that for the standard cell,  $\Delta FF_{J02}$  is within a relative error limit of 5% for  $J_{02}$  values up to  $10^{-7}$  A/cm<sup>2</sup>. For the high-efficiency cell, however, the relative error reaches 10% when  $J_{02}$  reaches  $10^{-7}$  A/cm<sup>2</sup>.

#### B. Approximation: $R_s$ Only Shifts $V_{mpp}$ and $R_{sh}$ Only Shifts $J_{mpp}$

The fill factor losses due to  $R_s$  and  $R_{sh}$  are calculated under this approximation. However, from the two-diode model, it can be seen that the presence of either  $R_s$  or  $R_{sh}$  shifts the MPP in terms of both current density and voltage (see Fig. 3).

We analyzed the error due to this approximation by comparing the fill factor losses due to  $R_s$  and  $R_{sh}$  calculated by (9) and (10) with the exact fill factor loss determined by the two-diode simulation. As in the previous section, we used the two sets of baseline parameters (see Table I) with an additional  $J_{02}$  term ( $J_{02} = 1.0 \times 10^{-9}$  A/cm<sup>2</sup>,  $n_2 = 2$ ) added to both baselines. The relative errors in  $\Delta FF_{R_s}$  and  $\Delta FF_{R_{sh}}$  are shown in Fig. 4.

For both the standard cell and the high-efficiency cell, the relative errors in  $\Delta FF_{R_s}$  and  $\Delta FF_{R_{sh}}$  are within the 5% limit for  $R_s < 4 \Omega \cdot \text{cm}^2$  and  $R_{sh} > 50 \Omega \cdot \text{cm}^2$ . The negative sign indicates that  $\Delta FF_{R_s}$  and  $\Delta FF_{R_{sh}}$  are underestimated. However, the error criteria for  $\Delta FF_{R_s}$  and  $\Delta FF_{R_{sh}}$  need to be more stringent

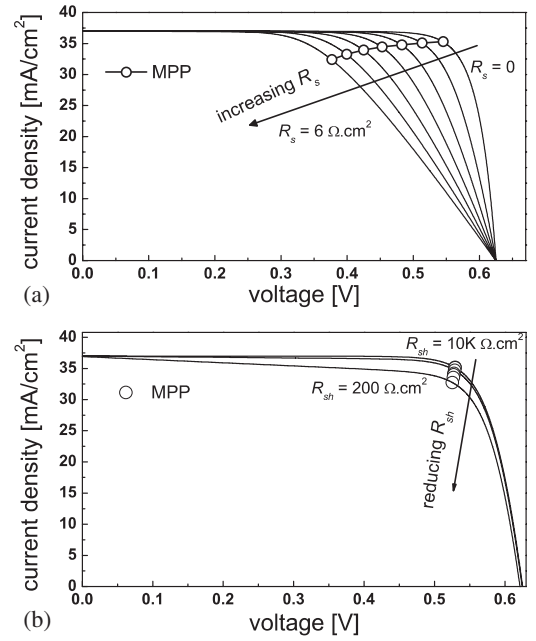


Fig. 3. Effect of (a) increasing  $R_s$  and (b) reducing  $R_{sh}$  on the  $J-V$  curve of solar cells. The curves were obtained by a two-diode simulation with baseline parameters  $J_{01} = 10^{-12}$  A/cm<sup>2</sup>,  $J_{02} = 10^{-9}$  A/cm<sup>2</sup>,  $n_2 = 2$ ,  $J_{ph} = 37$  mA/cm<sup>2</sup>,  $R_{sh} = 10 \text{ k}\Omega \cdot \text{cm}^2$  for (a) and  $R_s = 0.5 \Omega \cdot \text{cm}^2$  for (b). For clarity, some intermediate  $J-V$  curves have been omitted from (b), and only the MPPs are shown.

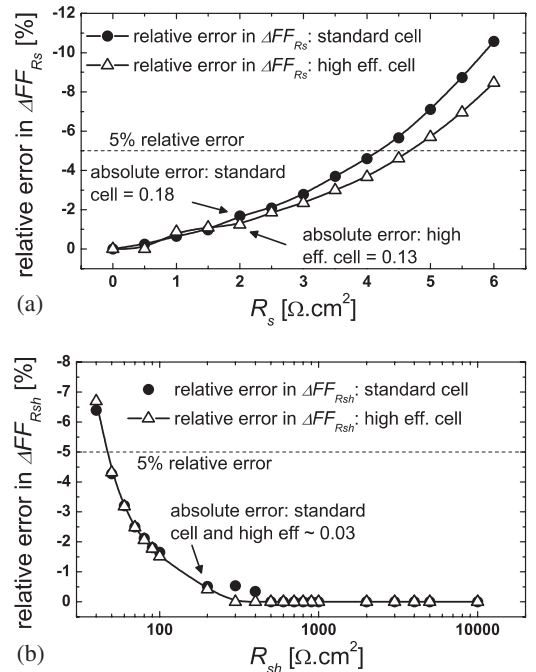


Fig. 4. Relative error in (a)  $\Delta FF_{R_s}$  as a function of  $R_s$  and (b)  $\Delta FF_{R_{sh}}$  as a function of  $R_{sh}$ .

because the error in these terms is transferred to  $\Delta FF_{J02}$  according to (8) and (11). If the absolute errors in  $\Delta FF_{R_s}$  and  $\Delta FF_{R_{sh}}$  are  $\delta(\Delta FF_{R_s})$  and  $\delta(\Delta FF_{R_{sh}})$ , respectively, then the absolute error in  $\Delta FF_{J02}$ ,  $\delta(\Delta FF_{J02})$  will be given by

$$\delta(\Delta FF_{J02}) = -\delta(\Delta FF_{R_s}) - \delta(\Delta FF_{R_{sh}}). \quad (12)$$

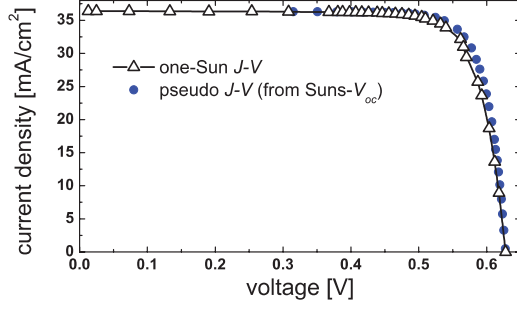


Fig. 5. 1-Sun  $J$ - $V$  curve and Suns- $V_{oc}$  curve of the inline-diffused cell.

Hence, we would like to ensure that the sum of the absolute errors in  $\Delta FF_{R_s}$  and  $\Delta FF_{R_{sh}}$  is limited to  $\sim 0.2$  (for all fill factor terms in %). This would be the case for  $R_s < 2 \Omega \cdot \text{cm}^2$  and  $R_{sh} > 200 \Omega \cdot \text{cm}^2$  for both the standard and the high-efficiency cell.

As a rule of thumb, the errors due to the approximations made in our fill factor loss analysis method will be small when  $R_s < 2 \Omega \cdot \text{cm}^2$ ,  $R_{sh} > 200 \Omega \cdot \text{cm}^2$ , and  $J_{02} < 10^{-7} \text{ A/cm}^2$ . This is likely to cover the entire practically important range of these quantities for silicon wafer solar cells.

#### IV. EXAMPLES OF APPLICATION OF THE METHOD

In this section, we demonstrate the application of the fill factor loss analysis method to an inline-diffused p-type silicon wafer solar cell and a heterojunction n-type silicon wafer solar cell.

##### A. Inline-Diffused p-Type Silicon Wafer Cell

The inline-diffused cell investigated here has a  $1.6 \Omega \cdot \text{cm}$  p-type Cz wafer base (area  $239 \text{ cm}^2$ ) and an  $n^+$  inline-diffused homogeneous emitter. Front and rear contacts were formed by screen printing and cofiring of a front silver grid (H pattern) and rear full-area aluminum contact. A detailed description of the inline diffusion process is given in [15]. The 1-Sun  $J$ - $V$  and the pseudo  $J$ - $V$  (from Suns- $V_{oc}$ ) curves of the cell measured on a 1-Sun flash tester (Sinton Instruments) are shown in Fig. 5, and the  $J$ - $V$  parameters are summarized in Table II.  $R_s$  at MPP was determined from the voltage shift at  $J_{mpp}$  between the 1-Sun  $J$ - $V$  curve and the Suns- $V_{oc}$  curve [10].  $R_{sh}$  was determined by the inverse of the slope of a linear fit to the cell's dark  $J$ - $V$  curve (not shown here) in the range 0–50 mV.  $pFF$  represents the pseudo fill factor obtained from the Suns- $V_{oc}$  curve (82.6%) which as expected closely matches the sum of the measured fill factor and the  $\Delta FF_{R_s}$  term (82.5%). Measurement of the Suns- $V_{oc}$  curve or the  $pFF$  is not necessary to apply the fill factor loss analysis since  $R_s$  at MPP may be obtained by other methods, e.g., 1) comparison of the 1-Sun  $J$ - $V$  curve and the shifted dark  $J$ - $V$  curve [13] and 2) comparison of two or more  $J$ - $V$  curves at different illumination intensities [1], [16].

The fill factor loss analysis of this solar cell reveals that  $FF_{J01}$  is 83.4%, and the drop to the cell's measured fill factor of 80.4% is primarily caused by series resistance (see Table II). The sources of series resistance of this cell were analyzed individually based on the unit cell approach of Mette [17]. The

parameters used for determining the series resistance components and the calculated series resistance components are summarized in Tables III and IV, respectively. All resistance components are within the limits expected from a screen-printed silicon wafer solar cell. The close match between the calculated sum of series resistance components and the measured  $R_s$  at MPP indicates optimized processing. Hence, without altering the present process flow, only a small improvement in fill factor can be expected via a lowering of the series resistance. A more effective route to improve the cell's fill factor is, therefore, to improve the shunt resistance and address the sources of  $J_{02}$  recombination. The shunt resistance can be improved by an optimization of the chemical edge isolation step used for this cell. To reduce  $J_{02}$  recombination, the inline diffusion step or the contact firing step may need further optimization.

We had earlier indicated our motivation to avoid fitting procedures to extract  $J_{01}$ ,  $J_{02}$ , and ideality factor. However, the Suns- $V_{oc}$  curve for the inline-diffused cell fits the two-diode model very well [see Fig. 6(a)], and it is possible to unambiguously determine parameters of the two-diode model ( $R_{sh}$  was fixed to the value determined earlier and  $J_{01}$ ,  $J_{02}$ , and  $n_2$  were fitted here). Hence, the fill factor loss terms for at least this cell can also be determined by simulation of the two-diode model based on measured and fitted parameters. This was done by simulating the  $J$ - $V$  curve with  $J_{01}$  alone and sequentially including  $J_{02}$ ,  $R_s$  (measured  $R_s$  at MPP), and  $R_{sh}$  to the  $J$ - $V$  curve [see Fig. 6(b)]. The results obtained [see Fig. 6(b)] agree exactly with the fill factor loss analysis results (see Table II). We also compared our fill factor loss analysis results (see Table II) with the Greulich/Hoenig approach [8], [9] (i.e.,  $\Delta FF_{R_{sh}}$  is assumed to be 0,  $\Delta FF_{R_s} = pFF - FF$ ,  $\Delta FF_{J02} = FF_{J01} - pFF$ ) which leads to  $FF_{J01} = 83.4\%$ ,  $\Delta FF_{R_s} = 2.2\%$ ,  $\Delta FF_{R_{sh}} = 0$ , and  $\Delta FF_{J02} = 0.8\%$ . The Greulich/Hoenig approach in this case overapproximates  $\Delta FF_{J02}$  by 0.2% absolute by ignoring the losses across  $R_{sh}$  and, hence, additionally attributing the fill factor loss across  $R_{sh}$  to  $J_{02}$ . This illustrates that the influence of  $R_{sh}$  should be considered for an accurate fill factor loss analysis. It is relevant to mention here that both our fill factor loss analysis and the Greulich/Hoenig approach are influenced in the same way by the approximation discussed in Section III-A. For the approximation discussed in Section III-B, the error (our analysis) in the inline-diffused cell's  $\Delta FF_{J02}$  term due to the  $R_s$  and  $R_{sh}$  ( $0.41 \Omega \cdot \text{cm}^2$  and  $4.3 \text{ k}\Omega \cdot \text{cm}^2$ ) is  $< 0.01\%$  absolute.

##### B. Heterojunction n-Type Silicon Wafer Solar Cell

The heterojunction silicon wafer solar cell that is investigated here (see Fig. 7) has a  $1 \Omega \cdot \text{cm}$  n-type FZ wafer base (active device area  $1.0 \text{ cm}^2$ ) with intrinsic amorphous silicon suboxides ( $a\text{-SiO}_x\text{:H}$ ) as interface passivation layers. A detailed discussion for this cell structure is given in [18]. The 1-Sun  $J$ - $V$  curve for the cell measured on a 1-Sun  $J$ - $V$  tester (steady-state light source, WACOM) and the Suns- $V_{oc}$  curve measured on a Sinton Suns- $V_{oc}$  tester are shown in Fig. 8, and the  $J$ - $V$  parameters are summarized in Table V.  $R_s$  at MPP and  $R_{sh}$  were determined using the same procedures mentioned earlier for the inline-diffused cell. The  $R_s$  value reported in [18] was determined



TABLE II  
1-SUN  $J$ - $V$  DATA AND FILL FACTOR LOSS ANALYSIS RESULTS FOR THE INLINE-DIFFUSED CELL

Cell parameters										FF loss analysis results			
Area (cm <sup>2</sup> )	$V_{oc}$ (mV)	$J_{sc}$ (mA/cm <sup>2</sup> )	FF (%)	Eff. (%)	$V_{mpp}$ (mV)	$J_{mpp}$ (mA/cm <sup>2</sup> )	$R_s$ at MPP ( $\Omega$ cm <sup>2</sup> )	$R_{sh}$ ( $\Omega$ cm <sup>2</sup> )	$pFF$ (%)	$FF_{J01}$ (%)	$\Delta FF_{R_s}$ (% absolute)	$\Delta FF_{R_{sh}}$ (% absolute)	$\Delta FF_{J02}$ (% absolute)
239	627.9	36.4	80.4	18.4	532.2	34.5	0.41	$4.3 \times 10^3$	82.6	83.4	2.1	0.3	0.6

TABLE III  
PARAMETERS USED TO CALCULATE SERIES RESISTANCE COMPONENTS

S. No	Parameter	Value
1	Front electrode design	79 fingers, 3 busbars
2	Wafer thickness (after texturing)	$\sim 170 \mu\text{m}$
3	Finger width	$90 \mu\text{m}$
4	Busbar width	1.5 mm
5	Emitter sheet resistance	$70 \Omega/\square$
6	Specific contact resistance	$1 \text{ m}\Omega\text{cm}^2$
7	Front metal paste sheet resistance	$1.8 \text{ m}\Omega/\square$

TABLE IV  
CALCULATED SERIES RESISTANCE COMPONENTS

Component	Front busbar	Front fingers	Front contact	Emitter	Base	Total
Resistance ( $\Omega\text{cm}^2$ )	0.02	0.09	0.03	0.22	0.03	0.39

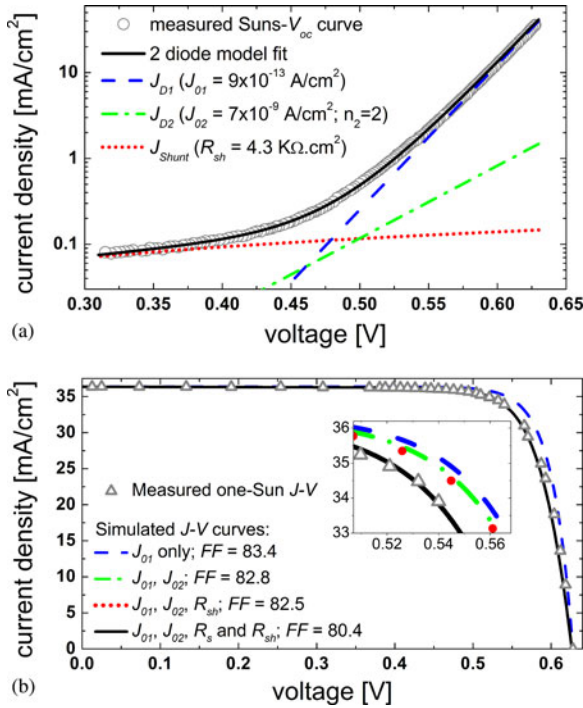


Fig. 6. (a) Two-diode model fit to the measured  $\text{Suns-}V_{oc}$  curve of the inline-diffused cell. (b) Simulated  $J$ - $V$  curves using measured and fitted parameters. For clarity, two intermediate  $J$ - $V$  curves are shown only in the inset.

from the slope of the 1-Sun  $J$ - $V$  curve at 800 mV; however, this is not an appropriate parameter for fill factor loss analysis and is not used here.

Due to the high  $V_{oc}$  of the heterojunction cell, it is important to check if the cell operates under LLI for most of the range between  $V_{mpp}$  and  $V_{oc}$ . An approximate check for LLI is to convert the quasi-Fermi level splitting under open-circuit con-

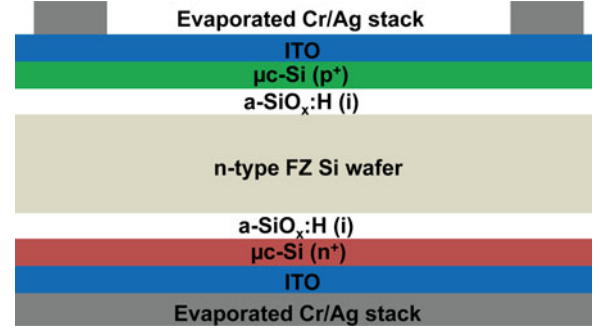


Fig. 7. Schematic of the heterojunction cell (texture omitted for clarity).

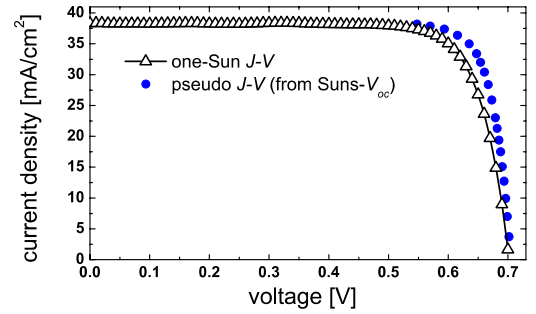


Fig. 8. 1-Sun  $J$ - $V$  curve and  $\text{Suns-}V_{oc}$  curve of the heterojunction cell.

ditions to injected carrier density ( $\Delta n$ ) and to compare this with the wafer doping ( $N_d$  for an n-type wafer). This leads to (13) if the cell is under LLI even under open-circuit conditions [19].  $n_i$  is the intrinsic carrier concentration for Si

$$V_{oc} < 2(kT/q) \ln[N_d/n_i]. \quad (13)$$

The  $1 \Omega\text{-cm}$  resistivity of the heterojunction cell corresponds to a doping of  $5 \times 10^{15} \text{ cm}^{-3}$ , and the term on the right side of (13) is 682 mV. Since  $V_{oc}$  of the heterojunction cell is 20 mV higher than this limit, the cell's bulk is likely to operate under the onset of high-level injection (HLI) conditions near open circuit. However, for most of the range between  $V_{mpp}$  (590 mV) and  $V_{oc}$  (702 mV), the bulk lies in LLI, and hence, the influence of this transition on fill factor is probably small and is not considered here. Application of the fill factor loss analysis indicates that  $FF_{J01}$  is 84.7%, and significant losses in fill factor are caused by  $R_s$  and  $J_{02}$  leading to a measured fill factor of 78.6%.  $R_{sh}$  for this heterojunction cell is very high, and no losses occur across it. Again, the sum of the measured fill factor and the  $\Delta FF_{R_s}$  term (83.4%) closely matches the  $pFF$  obtained from the  $\text{Suns-}V_{oc}$  curve (83.3%). Furthermore, the  $\text{Suns-}V_{oc}$  curve of the heterojunction also gave a reasonable fit to the two-diode model [see Fig. 9(a)], and we repeated the fitting and simulation procedure, as discussed earlier. The results obtained [see Fig. 9(b)] were

TABLE V  
1-SUN  $J$ - $V$  DATA AND FILL FACTOR LOSS ANALYSIS RESULTS FOR THE HETEROJUNCTION CELL

Cell parameters										FF loss analysis results			
Area (cm <sup>2</sup> )	$V_{oc}$ (mV)	$J_{sc}$ (mA/cm <sup>2</sup> )	$FF$ (%)	Eff. (%)	$V_{mpp}$ (mV)	$J_{mpp}$ (mA/cm <sup>2</sup> )	$R_s$ at MPP ( $\Omega$ cm <sup>2</sup> )	$R_{sh}$ ( $\Omega$ cm <sup>2</sup> )	$pFF$ (%)	$FF_{J01}$ (%)	$\Delta FF_{Rs}$ (%)	$\Delta FF_{Rsh}$ (% absolute)	$\Delta FF_{J02}$ (%)
1.0	702.2	38.3	78.6	21.1	590	35.8	1.0	$1 \times 10^6$	83.3	84.7	4.8	0.0	1.3

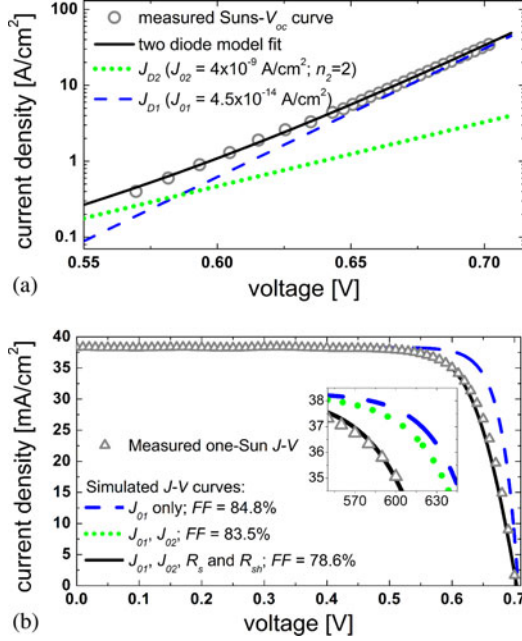


Fig. 9. (a) Two-diode model fit to the measured Suns- $V_{oc}$  curve of the heterojunction cell. (b) Simulated  $J$ - $V$  curves using measured and fitted parameters. For clarity, an intermediate  $J$ - $V$  curve is shown only in the inset.

in good agreement (all terms match within 0.1% absolute) with the fill factor loss analysis (see Table V). We again compared our results for the heterojunction cell with the Greulich/Hoening approach [8], [9], leading to  $FF_{J01} = 84.7\%$ ,  $\Delta FF_{Rs} = 4.7\%$ ,  $\Delta FF_{Rsh} = 0$ , and  $\Delta FF_{J02} = 1.4\%$ . In this case, as  $\Delta FF_{Rsh}$  is indeed zero, there is good agreement between these two approaches (all terms match within 0.1% absolute).

## V. DISCUSSION OF INJECTION-DEPENDENT EFFECTS

The fill factor loss analysis method presented in this paper is based on the two-diode model of solar cells, where we assume that  $J_{01}$  is not injection dependent and follows an ideality factor of 1. No assumptions are made about the ideality factor of the  $J_{02}$  term, and it may vary based on the source of  $J_{02}$  recombination. The conditions regarding  $J_{01}$  are valid under LLI in the absence of strong injection-dependent effects in the bulk and on the cell's two surfaces. The LLI condition can be verified for a cell by (13). If the bulk undergoes a transition from LLI to the onset of HLI close to  $V_{oc}$  (as was the case for the heterojunction cell discussed earlier), then this transition is only likely to have a small influence on fill factor. However, if the transition occurs close to  $V_{mpp}$ , then the fill factor will be additionally strongly affected by the onset of HLI. Other known injection-dependent effects that can influence fill factors (even when the LLI condition is fulfilled) are injection-dependent

bulk lifetimes in boron doped Cz or multicrystalline wafers due to boron-oxygen-related defects [20] and injection-dependent surface recombination at  $\text{SiO}_2$  passivated Si rear surfaces [21]. For cells affected by such injection-dependent effects, the  $\Delta FF_{J02}$  term calculated by our method will additionally include the influence of injection-dependent effects on fill factor, since this term is obtained directly by the difference between  $FF_{J01}$  and the resistance corrected  $FF_0$ . In such cases, the gap between  $FF_{J01}$  and the measured  $FF$  will be attributed to  $R_s$ ,  $R_{sh}$ , and the lumped effect of  $J_{02}$  recombination and injection-dependent effects on fill factor. Within the framework of this simple analysis, it is not possible to separate the influence of  $J_{02}$  recombination and injection-dependent effects on fill factor.

## VI. CONCLUSION

A method was described to analyze the fill factor losses of silicon wafer solar cells due to series resistance, shunt resistance, and  $J_{02}$  recombination. An error analysis revealed that the error due to the method's simplifying approximations is sufficiently small when  $R_s < 2 \Omega \cdot \text{cm}^2$ ,  $R_{sh} > 200 \Omega \cdot \text{cm}^2$ , and  $J_{02} < 10^{-7} \text{ A/cm}^2$ . This range is likely to cover the entire practically important range of these quantities for silicon wafer solar cells. Application of the fill factor loss analysis was demonstrated on an 18.4% efficient inline-diffused p-type silicon wafer solar cell and 21.1% efficient heterojunction n-type silicon wafer solar cell. It was further shown that if the two-diode model parameters can be unambiguously determined from a fitting of the cell's Suns- $V_{oc}$  curve, then the fill factor losses determined by simulation of the cell's diode models with measured and fitted parameters closely match the results of the fill factor loss analysis method presented here. Limitations of the method for solar cells strongly affected by injection-dependent effects were also discussed.

## APPENDIX

The Lambert W-Function [12]  $W$  is defined as the inverse function of the function  $f(x) = x \exp(x)$ . While there is no simple expression for  $W$ , it can be easily evaluated using mathematical software like Mathematica. The Lambert W-Function is useful to solve transcendental equations involving exponential terms and has been previously used for solar cell analysis to extract cell parameters from measured  $I$ - $V$  curves [22], [23]. Here, we will use this function to obtain an exact expression for  $FF_{J01}$ . We first define  $V_{mpp0}$ ,  $J_{mpp0}$  as the MPP for the hypothetical case when the absence of  $R_s$ ,  $R_{sh}$ , and  $J_{02}$  is assumed, i.e., the  $J_{01}$  limit described in Section II-A. In addition, from the definition of  $W$ , we note the following property, which will be subsequently used:

$$W[x \exp(x)] = x. \quad (\text{A1})$$

We start with the maximum power condition, i.e.,  $d(JV)/dV = 0$  at  $V = V_{\text{mpp}0}$ , and substitute  $J$  from (3). This leads to

$$J_{\text{sc}} \frac{d}{dV} \left[ V - \frac{V \{ \exp(qV/kT) - 1 \}}{\exp(qV_{\text{oc}}/kT) - 1} \right] = 0 \text{ at } V = V_{\text{mpp}0}. \quad (\text{A2})$$

Differentiating and setting  $V = V_{\text{mpp}0}$  yields

$$\exp(qV_{\text{oc}}/kT) = (1 + qV_{\text{mpp}0}/kT) \exp(qV_{\text{mpp}0}/kT). \quad (\text{A3})$$

Multiplying both sides by  $\exp(1)$ , we get

$$\exp(1 + qV_{\text{oc}}/kT) = (1 + qV_{\text{mpp}0}/kT) \exp(1 + qV_{\text{mpp}0}/kT). \quad (\text{A4})$$

We now use the terms on both sides of (A4) as arguments for the Lambert W-Function and use the property stated in (A1). This leads to

$$W[\exp(1 + qV_{\text{oc}}/kT)] = (1 + qV_{\text{mpp}0}/kT). \quad (\text{A5})$$

$FF_{J01}$  can now be computed as

$$FF_{J01} = (V_{\text{mpp}0} J_{\text{mpp}0}) / V_{\text{oc}} J_{\text{sc}}. \quad (\text{A6})$$

$J_{\text{mpp}0}$  is substituted from (3) with  $V = V_{\text{mpp}0}$ , and some simplification leads to

$$FF_{J01} = \left( \frac{V_{\text{mpp}0}}{V_{\text{oc}}} \right) \left[ \frac{\exp(qV_{\text{oc}}/kT) - \exp(qV_{\text{mpp}0}/kT)}{\exp(qV_{\text{oc}}/kT) - 1} \right]. \quad (\text{A7})$$

Substituting for  $\exp(qV_{\text{oc}}/kT)$  from (A3) yields

$$FF_{J01} = \left( \frac{qV_{\text{mpp}0}^2}{kTV_{\text{oc}}} \right) \left[ \frac{\exp(qV_{\text{mpp}0}/kT)}{\exp(qV_{\text{oc}}/kT) - 1} \right]. \quad (\text{A8})$$

Substituting for  $V_{\text{mpp}0}$  from (A5) leads to the expression for  $FF_{J01}$  using the Lambert W-Function, as previously stated in (4):

$$FF_{J01} = \frac{kT}{qV_{\text{oc}}} \cdot \frac{(W[z] - 1)^2 \exp(W[z] - 1)}{\exp(qV_{\text{oc}}/kT) - 1} \\ z = \exp[1 + qV_{\text{oc}}/kT]. \quad (\text{A9})$$

## REFERENCES

- [1] M. Wolf and H. Rauschenbach, "Series resistance effects on solar cell measurements," *Adv. Energy Convers.*, vol. 3, pp. 455–479, 1963.
- [2] W. Shockley and W. T. Read, "Statistics of the recombination of holes and electrons," *Phys. Rev.*, vol. 87, pp. 835–842, 1952.
- [3] R. N. Hall, "Electron-hole recombination in germanium," *Phys. Rev.*, vol. 87, pp. 387–387, 1952.
- [4] C. T. Sah, R. Noyce, and W. Shockley, "Carrier generation and recombination in p-n Junctions and p-n junction characteristics," *Proc. IRE*, vol. 45, pp. 228–1243, 1957.
- [5] K. McIntosh, "Lumps, humps and bumps: Three detrimental effects in the current-voltage curve of silicon solar cells," Ph.D. dissertation, Centre Photovolt. Eng., Univ. New South Wales, Sydney, Australia, 2001.
- [6] O. Breitenstein, J. P. Rakotonjaina, and M. H. Al Rifai, "Shunt types in crystalline silicon solar cells," *Prog. Photovolt.*, vol. 12, pp. 529–538, 2004.
- [7] S. Steingrube, O. Breitenstein, K. Ramspeck, S. Glunz, A. Schenk, and P. P. Altermatt, "Explanation of commonly observed shunt currents in c-Si solar cells by means of recombination statistics beyond the Shockley-Read-Hall approximation," *J. Appl. Phys.*, vol. 110, 014515, pp. 1–10, 2011.
- [8] J. Greulich, M. Glatthaar, and S. Rein, "Fill factor analysis of solar cells' current-voltage curves," *Prog. Photovolt.*, vol. 18, pp. 511–515, 2010.

- [9] R. Hoenig, M. Glatthaar, F. Clement, J. Greulich, J. Wilde, and D. Biro, "New measurement method for the investigation of space charge region recombination losses induced by the metallization of silicon solar cells," *Energy Procedia*, vol. 8, pp. 694–699, 2011.
- [10] R. Sinton and A. Cuevas, "A quasi-steady-state open-circuit voltage method for solar cell characterization," in *Proc. 16th Eur. Photovolt. Solar Energy Conf.*, Glasgow, U.K., 2000, pp. 1152–1155.
- [11] M. A. Green, "Accuracy of analytical expressions for solar cell fill factors," *Solar Cells*, vol. 7, pp. 337–340, 1982.
- [12] E. W. Weisstein. (2013, Jan.). Lambert W-Function, from Wolfram Math-World [Online]. Available: <http://mathworld.wolfram.com/LambertW-Function.html>
- [13] A. G. Aberle, S. R. Wenham, and M. A. Green, "A new method for accurate measurements of the lumped series resistance of solar cells," in *Proc. 23rd IEEE Photovolt. Spec. Conf.*, Louisville, KY, USA, 1993, pp. 133–138.
- [14] P. Cousins, D. Smith, H. Luan, J. Manning, T. Dennis, A. Waldhauer, K. Wilson, G. Harley, and W. Mulligan, "Generation 3: Improved performance at lower cost," in *Proc. 35th IEEE Photovolt. Spec. Conf.*, 2010, HI, USA, pp. 275–278.
- [15] P. K. Basu, M. B. Boreland, K. D. Shetty, D. Sarangi, and A. G. Aberle, "18.3% efficient inline diffused emitter silicon wafer solar cells," in *Proc. Tech. Dig. Photovolt. Solar Energy Conf. Exhib.*, Fukuoka, Japan, 2011.
- [16] K. C. Fong, K. R. McIntosh, and A. W. Blakers, "Accurate series resistance measurement of solar cells," *Prog. Photovolt.: Res. Appl.*, vol. 21, pp. 490–499, 2013.
- [17] A. Mette, "New concepts for front side metallization of industrial silicon solar cells," Ph.D. dissertation, Dep. Appl. Sci., Univ. Freiburg, Freiburg, Germany, pp. 16–17, 2007.
- [18] T. Mueller, J. Wong, and A. G. Aberle, "Heterojunction silicon wafer solar cells using amorphous silicon suboxides for interface passivation," *Energy Procedia*, vol. 15, pp. 97–106, 2012.
- [19] P. J. Verlinden, M. Aleman, N. Posthuma, J. Fernandez, B. Pawlak, J. Robbelein, M. Debucquoy, K. V. Wichelen, and J. Poortmans, "Simple power-loss analysis method for high-efficiency interdigitated back contact (IBC) silicon solar cells," *Solar Energy Mater. Solar Cells*, vol. 106, pp. 37–41, 2012.
- [20] K. Bothe, R. Sinton, and J. Schmidt, "Fundamental boron-oxygen-related carrier lifetime limit in mono- and multicrystalline silicon," *Prog. Photovolt.*, vol. 13, pp. 287–296, 2005.
- [21] A. G. Aberle, S. J. Robinson, A. Wang, J. Zhao, S. R. Wenham, and M. A. Green, "High-efficiency silicon solar cells: Fill factor limitations and non-ideal diode behaviour due to voltage-dependent rear surface recombination velocity," *Prog. Photovolt.*, vol. 1, pp. 133–143, 1993.
- [22] A. Jain and A. Kapoor, "Exact analytical solutions of the parameters of real solar cells using Lambert W-function," *Solar Energy Mater. Solar Cells*, vol. 81, pp. 269–277, 2003.
- [23] A. Jain and A. Kapoor, "A new method to determine the diode ideality factor of real solar cell using Lambert W-function," *Solar Energy Mater. Solar Cells*, vol. 85, pp. 391–396, 2005.



**Ankit Khanna** received the Master of Technology degree in engineering physics from the Indian Institute of Technology (Banaras Hindu University), Varanasi, India, in 2010. Since 2011, he has been working toward the Ph.D. degree with the Solar Energy Research Institute of Singapore, Singapore, focusing on metallization methods for silicon wafer solar cells.



**Thomas Mueller** received the Diploma degree in electrical engineering from the University of Dortmund, Dortmund, Germany, and the Ph.D. degree from the University of Hagen, Hagen, Germany.

He is the Head with the Silicon Wafer Solar Cells I Group of the Solar Energy Research Institute of Singapore, Singapore. His research focuses on advanced high-efficiency silicon wafer solar cell architectures such as all-back-contact and heterojunction cells.



**Rolf A. Stangl** received the Ph.D. degree in organic solar cells for work conducted with the Fraunhofer Institute for Solar Energy Systems, Freiburg, Germany.

He is a Senior Research Scientist with the Solar Energy Research Institute of Singapore, Singapore. He is a Project Leader for hybrid heterojunction solar cells and a competence Team Leader for electrical characterization/simulation.



**Prabir K. Basu** received the B.Sc./M.Sc./M.S. and Ph.D. degrees in physics from several universities in India.

He is a Senior Research Scientist with the Solar Energy Research Institute of Singapore, National University of Singapore, Singapore. His research focuses on low-cost industrial high-efficiency silicon wafer solar cells.



**Bram Hoex** received the M.Sc. and Ph.D. degrees in applied physics from the Eindhoven University of Technology, Eindhoven, The Netherlands.

He is a Director and Group Leader with the Silicon Materials and Cells Cluster, Solar Energy Research Institute of Singapore, Singapore. His research focuses on advanced fabrication and characterization of high-efficiency silicon wafer solar cells.



**Armin G. Aberle** received the Physicist and Ph.D. degrees in physics from the University of Freiburg, Freiburg, Germany, in 1988 and 1992, respectively, and the Dr. rer. nat. habil. degree in physics from the University of Hannover, Hannover, Germany, in 1999.

He is the Chief Executive Officer with the Solar Energy Research Institute of Singapore, Singapore. He has published extensively (>300 papers), and his work has a high impact (>4000 citations). He is an Editor of several scientific journals. In the 1990s, he

established the Silicon Photovoltaics (PV) Department at the Institute for Solar Energy Research Hamelin, Hamelin, Germany. He then worked for 10 years in Australia as a Professor of PV with the University of New South Wales, Sydney.